

Energy dependence of the charge asymmetry $A(T_\pi, \theta)$ in πd elastic scattering

G. R. Smith, D. R. Gill, D. Ottewell, G. D. Wait, and P. Walden
TRIUMF, Vancouver, British Columbia, Canada V6T 2A3

R. R. Johnson, R. Olszewski, R. Rui,* M. E. Sevier, and R. P. Trelle
University of British Columbia, Vancouver, British Columbia, Canada V6T 1W5

J. Brack, J. J. Kraushaar, R. A. Ristinen, and H. Chase
Nuclear Physics Laboratory, Department of Physics, University of Colorado, Boulder, Colorado 80309

E. L. Mathie and V. Pafilis
University of Regina, Regina, Saskatchewan, Canada S4S 0A2

R. B. Schubank and N. R. Stevenson
University of Saskatchewan, Saskatoon, Saskatchewan, Canada S7N 0W0

A. Rinat and Y. Alexander
Department of Physics, Weizmann Institute of Science, 76100 Rehovot, Israel
 (Received 8 September 1987)

Angular distributions of charge asymmetry $A(T_\pi, \theta)$, have been measured for πd elastic scattering. Data were obtained in the backward hemisphere for pion bombarding energies of 143, 180, 220, and 256 MeV. The results are compared with predictions employing different mass and width parameters for the delta isobars.

I. INTRODUCTION

An increasing number of experimental and theoretical efforts in the last few years have focused on πd elastic scattering. Valuable new information on this fundamental reaction has recently been obtained by measurements of the vector analyzing power iT_{11} ,¹ the tensor analyzing power T_{20} ,² and the tensor polarization t_{20} .^{3,4,5} These spin observables provide important tests for sophisticated three body theories of the πNN system, and have raised many fascinating new questions.

In addition, several experiments have been performed which measure the difference between π^+d and π^-d cross sections, and which relate to the question of charge symmetry breaking (CSB). Charge symmetry (CS) manifests itself in its simplest form in systems which are in a unique state of total isospin T and have opposite values of T_3 . CS implies that for every observable B , $B(T, T_3) = B(T, -T_3)$. In particular, for the $T=1$ πd system, $T_3 = +1$ for π^+d and $T_3 = -1$ for π^-d . After removal of electromagnetic effects, therefore, $B'(\pi^+d)$ should be the same as $B'(\pi^-d)$. In the πd system, described by hadronic degrees of freedom, CS is ensured if proton and neutron masses are equal and if πN amplitudes for a given T are independent of T_i .

Observed CSB effects may be studied on the hadronic level or using subhadronic degrees of freedom. The former is evidently the simplest, i.e., one considers differing neutron and proton masses, and T_3 dependent pion-nucleon amplitudes. With P_{33} the dominant πN channel,

a measure for the T_3 dependence is provided by the different masses and widths of the delta isobars Δ^- , Δ^0 , Δ^+ , and Δ^{++} . For attempts to relate these differences to the mass difference of the u and d quarks, see Ref. 6.

We report below new, precise measurements of the charge symmetry $A(T_\pi, \theta)$ for πd elastic scattering at four bombarding energies spanning the region of the (3,3) resonance. The experiment was performed on the M11 beamline at TRIUMF. Typically twelve angles have been measured in the backward hemisphere at each bombarding energy. Results from previous experiments are summarized in Sec. II. After describing the experimental technique used for these measurements in Sec. III, we present our results in Sec. IV. We describe the results of a theoretical analysis in Sec. V, and formulate our conclusions in Sec. VI.

II. PREVIOUS EXPERIMENTS

The first tests of charge symmetry in the πd system consisted of precise measurements of π^+d and π^-d total cross sections between 70 and 370 MeV.⁷ Differences were observed in this experiment at the 3–8% level, which persist after Coulomb and Coulomb-nuclear interference corrections are included. After applying these electromagnetic corrections, a larger total cross section was found for π^+d than for π^-d below the (3,3) resonance region, and a smaller total cross section for π^+d than for π^-d above the resonance. The results were parametrized in terms of mass and width differences

among the charge components of the Δ isobar, using the well-known measures for CSB

$$\begin{aligned} C_M &= (M_- - M_{++}) + \frac{1}{3}(M_0 - M_+), \\ C_\Gamma &= (\Gamma_- - \Gamma_{++}) + \frac{1}{3}(\Gamma_0 - \Gamma_+). \end{aligned} \quad (1)$$

The best agreement with the total cross section measurements was obtained with $C_M = 4.6 \pm 0.2$ MeV and $C_\Gamma = 3.6 \pm 0.3$ MeV. Note that the mass difference parameter C_M is sometimes referred to as C_W in earlier publications.^{7,8,9}

Stimulated in part by these results, a measurement of charge asymmetry $A(143, \theta)$ in πd elastic scattering was performed at LAMPF.⁸ This measure is defined in terms of the differential cross sections σ^\pm for $\pi^\pm d$ elastic scattering at a given pion bombarding energy T_π (in MeV), and c.m. scattering angle θ according to

$$A(T_\pi, \theta) = \frac{\sigma^-(\theta) - \sigma^+(\theta)}{\sigma^-(\theta) + \sigma^+(\theta)}. \quad (2)$$

The angular range of this experiment was $22^\circ \leq \theta_{\text{lab}} \leq 120^\circ$. The incident energy of $T_\pi = 143$ MeV was chosen to coincide with the maximal deviation from charge symmetry observed in the total cross-section measurements of Ref. 7. An average uncertainty of $\pm 1.5\%$ was obtained in these results, a remarkable achievement considering the fact that the data were collected in a single arm experiment with a CD_2 target and the EPICS pion spectrometer. Normally this device is capable of only 10–15% uncertainties in measured cross sections. However, many experimental uncertainties cancel out, since $A(T_\pi, \theta)$ consists of a ratio of cross sections. Nevertheless, the results of Ref. 8 had to be normalized by measuring $\pi^\pm p$ relative cross sections, and using them in conjunction with $\pi^\pm p$ absolute cross sections predicted from a phase shift program. Depending on which set of available phase shifts was used, the resulting $\pi^\pm d$ cross sections of Ref. 8 differed by as much as 8%. Clearly this is a serious limitation of the pion spectrometer technique used in the experiment of Ref. 8. We shall come back to this point in Sec. IV, where the impact of different $\pi^\pm p$ normalizations on the results of the Ref. 8 experiment is discussed in a comparison to the results of the present experiment.

The results of the Masterson *et al.* experiment,⁸ when parametrized in terms of the global quantities of Eq. (1), gave $C_M = 4.35 \pm 0.50$ MeV and $C_\Gamma = 0$ MeV in their first publication. A subsequent, and more sophisticated analysis presented in their second publication⁹ resulted in the values $C_M = 3.1 \pm 1.1$ MeV and $C_\Gamma = 1.24$ MeV. For comparison, the value found from the total cross-section results of Ref. 7 is $C_M = 4.6 \pm 0.2$ MeV. An analysis using more detailed information than available in the global parameters of Eq. (1) will be presented in Sec. V.

An interesting feature of the data of Ref. 8 was the existence of a bump in $A(143, \theta)$ near 100° . This bump could not be explained in terms of mass or width parameters of the Δ isobar. The authors of Ref. 8 suggested that measurements at $T_\pi = 180$ MeV would be useful in understanding the nature of this enhancement. At the bench-

mark bombarding energy of $T_\pi = 180$ MeV, only minimal effects due to changes in C_M were foreseen.¹⁰

The question of the bump in the data of Ref. 8 received additional significance after a measurement of $A(65, \theta)$ was reported.¹¹ These lower-energy data showed a very definite bump in the same angular region as observed in the $T_\pi = 143$ MeV data. An impulse approximation calculation did not reproduce the bump in the $A(65, \theta)$ results,¹¹ whereas a refined treatment of pure Coulomb effects as well as the charge extension of the pion and deuteron did so for $A(143, \theta)$ but not for $A(65, \theta)$.¹² The present work was undertaken to investigate the existence of the $T_\pi = 143$ MeV bump, and to explore the energy dependence of $A(T_\pi, \theta)$.

Above the (3,3) resonance, Pedroni *et al.*⁷ observed a deviation from charge symmetry in $\pi^\pm d$ total cross sections opposite to that observed at 143 MeV. The effect was maximal near $T_\pi = 250$ MeV. Measurements of $A(256, \theta)$ were thus performed by Masterson *et al.*⁹ using the same experimental technique they employed for the $A(143, \theta)$ measurements. Their analysis of the $A(256, \theta)$ results revealed considerably less sensitivity to the mass and width parameters C_M and C_Γ relative to that seen at 143 MeV. Values of C_M between 2 and 4.5 MeV were consistent with their measurements of $A(256, \theta)$, and almost no sensitivity to C_Γ was observed. Although the quality of the $A(256, \theta)$ results was somewhat worse than the quality of the $A(143, \theta)$ results, no evidence for a bump near 100° was found at 256 MeV.

III. EXPERIMENTAL PROCEDURE

The detection system used in the present experiment for measurements of $A(T_\pi, \theta)$ in the πd elastic scattering reaction is similar to systems used for measurements of iT_{11} and T_{20} (Refs. 1 and 2) in this reaction, and is shown in Fig. 1. A solid angle of 27 msr for each of six independent arms was defined by a two element pion telescope. The pion telescopes each consisted of a plastic scintillator $(\pi 2)_i$ located 1.0 m from the deuteron target, and another plastic scintillator $(\pi 1)_i$ at a radius of 0.5 m.

Each pion telescope was placed in coincidence with an associated recoil deuteron arm consisting of three plastic scintillators. The first scintillator $(D 1)_i$ at a radius of 1.3 m from the target was a thin (3 mm) scintillator which provided TOF as well as energy loss information. Following this scintillator was an aluminum absorber, whose thickness was adjusted so that deuterons would stop in the following 13 mm thick scintillator $(D 2)_i$. The third was a veto scintillator $(D 3)_i$.

The incident beam was counted directly with scintillators $S 1$ and $S 2$ in coincidence. The incident flux varied depending on the polarity of the beam and the bombarding energy, but was typically 2×10^6 π /sec. Protons in the incident π^+ beam were reduced by using a differential degrader near the midplane of the $M 11$ channel. This degrader was left in place for the π^- data collection as well. Protons remaining in the π^+ beam were eliminated by placing pulse height vetoes on $S 1$ and $S 2$ in the trigger, defined by

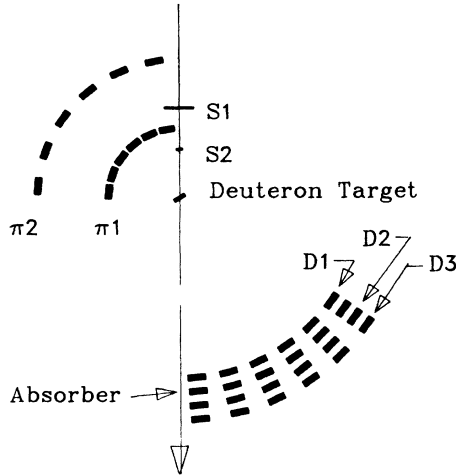


FIG. 1. The experimental layout is shown, with the pion beam incident from the top. The meaning of the various detector rings is explained in the text.

$$S1 \cdot S2 \cdot \overline{S1} \cdot \overline{S2} \cdot (\pi 1)_i \cdot (\pi 2)_i \cdot (D1)_i \cdot \overline{(D3)}_i .$$

The size of $S2$ was chosen such that its image at the target would be smaller than the target itself. A three element monitor telescope viewed the scattering target, providing a relative monitor of the incident flux as a consistency check. A horizontally and vertically split scintillator several meters downstream of the scattering target was used as a relative monitor of the spatial stability of the incident beam. This device was sensitive to shifts of as little as $100 \mu\text{m}$ in the incident beam position on the scattering target. The horizontal and vertical divergences of the beam were less than 1° . The momentum acceptance of the channel was kept fixed for a given angular setting of the detectors. The momentum acceptance $\Delta p/p$ (FWHM) was 1.1% at 143 MeV , and 3.3% at 256 MeV . For bombarding energies of 180 and 220 MeV the momentum acceptance was 1.1% for one angular setting and 1.7% for another angular setting. The mean incident pion energies at the center of the scattering target were 142.8 , 179.3 , 220.0 , and 256.1 MeV . These energies are accurate to $\pm 0.3 \text{ MeV}$.

The targets used for the studies were solid plastic slabs of CD_2 , with an isotopic deuterium purity $> 99\%$. Two targets were available, with areal densities of 224 mg/cm^2 and 405 mg/cm^2 . At $T_\pi = 256 \text{ MeV}$, both targets were used (stacked together). At the other three energies of this experiment, the 405 mg/cm^2 target was used. Explicit measurements of the small background from quasi-free πd elastic scattering on carbon were made using graphite slab targets. The areal densities of the two graphite targets used in conjunction with the CD_2 targets above were 344 mg/cm^2 and 686 mg/cm^2 . The angle of the targets with respect to the incident beam was always 30° .

The data were collected in sequences of positive and negative beam polarity, in order to minimize possible systematic errors. Each sequence included three π^+ and

three π^- runs, as well as three changes of the incident beam polarity. A typical beam polarity sequence was $\pi^- \pi^+ \pi^- \pi^+ \pi^- \pi^+$. A π^- background measurement would precede this sequence, and a π^+ background measurement would follow this sequence. These measurements of the background yield from the carbon (graphite) target were made for each beam polarity at the beginning and end of the sequence to ensure that the foreground (CD_2) scattering target remained untouched for the duration of the data collection for a given sequence. This is an important feature, because in principle a slight change of the target position or angle between π^+ and π^- data collection could have had a serious impact on the measured $A(T_\pi, \theta)$.

The relative differential cross sections were calculated from measurements of the πd elastic scattering yield $N_{\pi d}$, the number of incident beam particles N_b counted in $S1$ and $S2$, the computer efficiency ϵ_{CPU} (typically 99%), the correction for multiple particles in the beam burst ϵ_{doub} , and the pion fraction of the incident beam f_π , according to

$$\sigma = \frac{N_{\pi d} \epsilon_{\text{doub}}}{N_b \epsilon_{\text{CPU}} f_\pi} . \quad (3)$$

The statistical uncertainty associated with the relative cross sections was $\leq 1\%$ for each sequence.

The correction factor ϵ_{doub} is necessary because the in-beam scintillators only count once regardless of how many particles there actually were in a given beam burst. At TRIUMF, the beam bursts are approximately 2.5 ns wide. They occur every 43 ns . The correction factor for TRIUMF (with a 100% duty cycle) is therefore

$$\epsilon_{\text{doub}} = \frac{\mu}{\ln \frac{1}{1-\mu}} \quad (4)$$

where

$$\mu = \frac{\text{measured incident flux}}{\text{cyclotron rf frequency}} .$$

At TRIUMF, the cyclotron rf frequency is 23 MHz . The measured incident flux corresponds to the number of coincidences per second counted in the beam scintillators $S1$ and $S2$. Upper level threshold requirements on these scintillators prevented beam protons from contributing to this flux. The doubles correction for a typical incident flux of $2 \times 10^6 \pi/\text{sec}$ is therefore 0.956 . The uncertainty associated with this correction increases as the incident flux increases. Therefore, the incident flux was constrained to be less than 3 MHz using the $M11$ vertical intensity slits. Even at this rate, assuming a 10% uncertainty in determining the incident flux, the uncertainty of this correction is only 0.7% . The scalers were inhibited and the experimental trigger disabled whenever the incident beam rate fell below 0.1 MHz .

Careful studies were made to check for any possible rate dependence in the measured $\pi^+ d$ cross sections. In particular, one worries about the possible systematic errors associated with changing the opening of the vertical intensity slits. These slits were varied during the experi-

ment to adjust the incident flux. Conceivably, changing these slits could affect the size of the pion beam spot, the angular divergence and incoming angle of the incident beam. To check the consequences of these possible effects, the incident flux was varied between 0.8 and 5.6 MHz using the *M11* vertical intensity slits. Although the cross sections obtained at 5.6 MHz appeared to be about 1.5% higher than the cross sections obtained at the other rates, there was no discernible rate dependence in the range of incident flux between 0.8 and 3.5 MHz, where the $A(T_\pi, \theta)$ measurements were acquired.

A further study was undertaken to study the possible influence of different pion production targets on the measured πd cross sections. Four pion production targets were available, a 10-mm-thick graphite target, a 2-mm-thick graphite target, a 12-mm-thick beryllium target, and a 10-mm-thick H_2O target. Because the *M11* production target is shared with two other beam lines, it was not possible to run with the thin 2 mm graphite target. However, it was possible to compensate partially for the different π^+ and π^- fluxes by changing the pion production target from 10 mm H_2O to 12 mm beryllium for π^+ and π^- beams, respectively. For example, at 320 MeV/ c , the ratio of π^+ to π^- fluxes (for a fixed setting of the channel slits and jaws) would be 25 if the H_2O production target had been used for both polarities. By employing the beryllium production target for the π^- measurements, however, this ratio is reduced to six. Test runs for which $\pi^+ d$ cross sections were measured using the various pion production targets were consistent with each other, as expected.

Ideally one could utilize this unique feature of TRIUMF to obtain similar pion fluxes for π^+ and π^- by changing just the production target, and nothing else. Unfortunately, pion production for the two polarities is dissimilar enough for higher pion energies that the channel slits must be changed as well to keep the fluxes for both π^+ and π^- confined to a reasonable range (between 1 and 3 MHz). At $T_\pi = 143$ MeV, the channel slits for each pion polarity were not changed. The resulting π^- and π^+ fluxes were 0.8 and 2.7 MHz, respectively. For the other three bombarding energies studied in this experiment, the channel (intensity) slits were opened wider for π^- data acquisition than for π^+ data acquisition. The resulting (average) π^+ and π^- incident fluxes were respectively 3.1 and 2.5 MHz at $T_\pi = 180$ MeV, 3.2 and 1.6 MHz at $T_\pi = 220$ MeV, and 2.8 and 1.0 MHz at $T_\pi = 256$ MeV.

The pion fraction of the incident beam f_π (see Table I) is the largest correction to the data which is sensitive to the incident beam polarity. For example, f_π is about 10% less for π^- than for π^+ at $T_\pi = 143$ MeV, but only about 1% less at $T_\pi = 256$ MeV. Considerable attention was therefore given to an accurate determination of this correction. During each run, the electron contamination of the incident beam was acquired (by means of a sample circuit) simultaneously with the $\pi^\pm d$ data. This was done by digitizing a timing signal from a capacitive probe in the TRIUMF proton beam line with respect to scintillator *S2*, located just upstream of the CD_2 scattering target. This timing signal therefore represents the TOF of

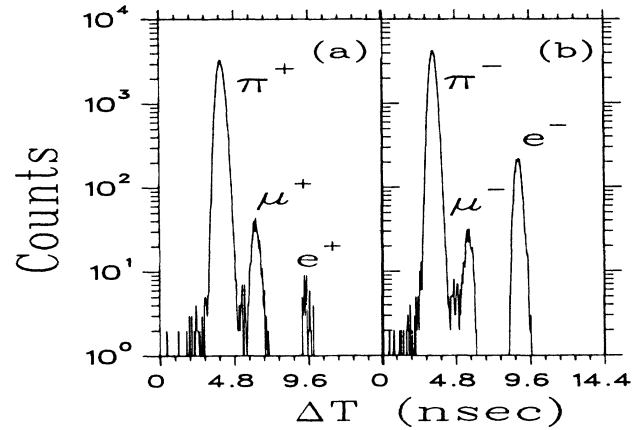


FIG. 2. The TOF spectrum of particles down the *M11* channel is shown for (a) positive and (b) negative beam polarities at $T_\pi = 180$ MeV. From left to right the peaks correspond to pions, muons and electrons or positrons. The separation between the pion and electron peaks is 5.7 ns.

particles from the *M11* production target down the (~ 14 m long) *M11* channel, smeared out by the instrumental (~ 0.5 ns) timing resolution and the width of the incident beam bucket (~ 2.5 ns). While this is sufficient for separation of electrons or positrons from the pions and muons, it is not sufficient for separation of muons from pions. On the one hand, it is hard to come up with a mechanism which would alter the muon contamination of the beam in a polarity dependent way. On the other hand, the $A(T_\pi, \theta)$ measurements would be critically sensitive to such a dependence. Therefore, a separate measurement of the incident beam fraction was made after the experiment, by limiting the phase space of the incident beam using slits in the TRIUMF cyclotron, such that the width of the incident beam buckets was ~ 0.6 ns, instead of the usual 2.5 ns. This made it possible to separate π^\pm , μ^\pm , and e^\pm at each of the bombarding energies studied in this experiment. The e^\pm contamination obtained in this special measurement was consistent with

TABLE I. The constituents of the incident pion beam are tabulated at each of the energies studied in this experiment. The numbers refer to the ratio of particles of a given type to the total number of particles of all types. The measurements were obtained using rf referenced TOF and a 0.6-ns-wide proton beam bucket as discussed in the text.

T_π (MeV)	Polarity	f_π	f_μ	f_e
143	π^+	0.977	0.018	0.005
	π^-	0.887	0.011	0.102
180	π^+	0.986	0.012	0.002
	π^-	0.942	0.008	0.050
220	π^+	0.990	0.007	0.002
	π^-	0.970	0.006	0.025
256	π^+	0.995	0.005	0.001
	π^-	0.985	0.005	0.009

that obtained from the earlier measurements with the wider beam bucket, which confirms the reliability of the former approach for obtaining the (small) muon contaminations. A typical spectrum (obtained using the narrow beam bucket) showing the separation of π^\pm , μ^\pm , and e^\pm at $T_\pi = 180$ MeV is presented in Fig. 2. Table I summarizes the results of the beam fraction studies with the narrow beam bucket measurements. The pion beam fractions listed there were used for the determination of $A(T_\pi, \theta)$.

The final analysis of the data was performed by constructing polygons around the πd elastic events identified in two-dimensional histograms of the deuteron TOF versus the deuteron total energy $E + \Delta E$, where ΔE corresponds to the pulse height in $D1$, and E to the pulse height in $D2$. A typical (foreground) scatterplot of these quantities is shown in Fig. 3. For a given setting of the detector angles and bombarding energy, the same polygons were used to obtain the π^+ and π^- foreground and background yields. The background amounted to typically 5% of the foreground yield.

The uncertainty in $A(T_\pi, \theta)$ includes the statistical uncertainties in the relative cross sections (typically $\leq 1\%$), as well as the statistical uncertainties associated with the determination of the incident pion beam fraction, the computer efficiency, and the correction for multiple particles within a given beam burst.

Precise measurements of the π^+d differential cross sections have recently been published¹³ for this energy regime. Our experimental configuration was therefore optimized for a measurement of relative $\pi^\pm d$ cross sections in order to obtain the best possible measurement of the charge asymmetry $A(T_\pi, \theta)$. Consequently, no absolute cross sections will be presented from this experiment. Consistency checks performed periodically during the

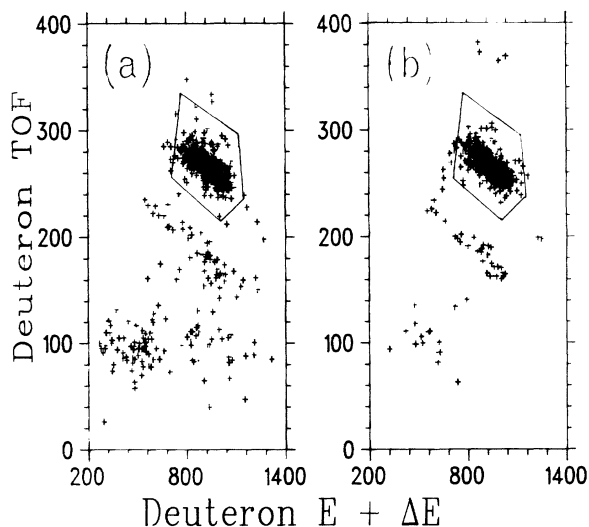


FIG. 3. A typical two-dimensional spectrum for π^+ (a) and π^- (b) of the deuteron TOF vs the sum of the deuteron pulse heights in the ΔE counter ($D1$) and the E counter ($D2$) is shown. This example is for $T_\pi = 180$ MeV and $\theta_{c.m.} = 140^\circ$. The deuteron band is enclosed by the polygon. The other events are protons from quasielastic scattering, absorption, and deuteron breakup reactions.

course of the experiment did indicate, however, that our measured absolute cross sections were in agreement with those of Ref. 13.

IV. EXPERIMENTAL RESULTS

The asymmetries measured in this experiment [according to Eq. (2)] have not been corrected for radiative effects. Such corrections, which differ slightly for π^+d and π^-d , arise due to the bremsstrahlung radiation associated with πd elastic scattering. Radiative corrections were calculated for the experiment of Masterson *et al.*^{8,9} using the relationships given by Borie.¹⁴ They depend on the pion scattering angle, the pion polarity and energy, and the energy acceptance of the detection system, and amounted to between -0.1 and -1.0 in corrections to the asymmetry (expressed in percent) in those experiments.

Knowledge of the energy acceptance is required in single-arm spectrometer experiments because photon emission modifies the energy of the outgoing particles. If the outgoing particle energy is modified outside the range of accepted particle energies, the event is lost, and the corresponding cross section is underestimated. The broader the energy acceptance of the experiment, the less the radiative correction becomes since more of the radiative distribution is included in the analysis.

It is not trivial to make radiative corrections in the present situation in which the scattered pion and recoil deuteron are detected in a coincidence experiment with plastic scintillation counters. Although the energy acceptance of these detectors is large (> 25 MeV), bremsstrahlung radiation may also influence the scattered or recoil particle angles. Kinematic correlations sufficiently complicate the phase-space integrations involved in calculation of the radiative corrections that a general expression cannot be obtained.¹⁵ For this reason, computation of the radiative correction is beyond the scope of the present work. However, approximate calculations indicate that the deflections of the particles from their kinematically correct angles due to bremsstrahlung radiation are no greater than about 0.5° at 143 MeV. For these reasons, we have not included radiative corrections in the asymmetries measured in this experiment.

Each of the measured asymmetries in this experiment is tabulated in Table II. The uncertainties listed in Table II include all known sources of uncertainty in the experiment, namely those associated with counting statistics, the beam pion fraction determination, the doubles correction to the incident flux, and the computer efficiency.

As mentioned previously, the asymmetries measured by Masterson *et al.*^{8,9} include radiative corrections. In that experiment the corrections were applied to their measured $\pi^\pm d$ cross sections as well as to their measured $\pi^\pm p$ cross sections. (The ratio of measured $\pi^\pm p$ cross sections to those predicted from a partial wave analysis program was used to normalize their $\pi^\pm d$ results.) The dominant contribution to their overall radiative correction arose from the correction to the measured $\pi^\pm p$ data. However, the data used to generate the $\pi^\pm p$ phase shifts (and corresponding cross sections) were not corrected for radiative effects. Furthermore, it is not clear how one

TABLE II. The results of this experiment are tabulated. All $A(T_\pi, \theta)$ and $\Delta A(T_\pi, \theta)$ values are in percent. The tabulated uncertainties $[\Delta A(T_\pi, \theta)]$ include all known sources of uncertainty, as discussed in the text. The column labeled Set refers to the detector setting in which data at six angles were acquired simultaneously.

T_π	$\theta_{c.m.}$	A (%)	ΔA (%)	Set	
143	92.7	0.73	0.87	1	
	107.6	-0.97	0.63	1	
	121.9	-0.46	0.60	1	
	135.8	-1.61	0.64	1	
	149.3	-1.72	0.64	1	
	162.5	-2.11	0.65	1	
	100.2	-1.29	0.76	2	
	114.8	-3.02	0.64	2	
	128.9	-0.63	0.63	2	
	142.6	-1.39	0.67	2	
	155.9	-0.74	0.68	2	
	166.9	-1.48	0.68	2	
	180	86.0	-1.14	0.59	1
		103.6	-0.73	0.61	1
115.6		-1.51	0.63	1	
125.0		-0.64	0.67	1	
140.9		-1.71	0.74	1	
158.5		-1.63	0.90	1	
78.3		-0.51	0.70	2	
96.2		-1.33	0.61	2	
115.6		-2.52	0.64	2	
131.9		-2.38	0.69	2	
149.7		-1.45	0.77	2	
167.1		-1.40	0.86	2	
78.3		-1.77	0.49	3	
96.1		-0.61	0.36	3	
115.6		-2.74	0.39	3	
131.9		-1.22	0.43	3	
149.7		0.37	0.47	3	
167.1		-2.59	0.52	3	
220	68.5	-0.70	0.45	1	
	84.4	0.12	0.58	1	
	104.4	-1.07	0.72	1	
	123.4	-0.04	0.78	1	
	141.4	-0.49	0.83	1	
	158.8	-1.85	0.82	1	
	76.5	-0.64	0.48	2	
	94.5	0.11	0.69	2	
	114.0	-0.16	0.76	2	
	132.5	-2.68	0.83	2	
	150.2	-0.14	0.97	2	
	167.3	2.42	1.04	2	
	256	69.3	-2.37	0.66	1
		90.3	-3.29	1.26	1
128.6		1.04	1.91	1	
146.3		-0.99	1.70	1	
163.3		1.23	1.29	1	
69.3		-1.74	0.62	2	
79.9		-2.35	0.92	2	
100.3		0.05	1.56	2	
119.4		0.40	1.65	2	
137.5		-6.93	1.81	2	
154.8		0.14	1.58	2	

would apply radiative corrections to those data since the required information on the energy acceptance of the detection system is not available. Forming the ratio between measured $\pi^\pm p$ cross sections which include radiative corrections, and predicted $\pi^\pm p$ cross sections based on data which do not include radiative corrections, is questionable. There is no easy way to know what the actual radiative correction should be in that experiment,^{8,9} because that would involve correcting the entire data base employed in the partial wave analysis by amounts which depend on the energy acceptance of each experiment (which is in general not reported).

The $A(T_\pi, \theta)$ results from the present experiment are displayed in Fig. 4 for each of the bombarding energies studied. The previously published data of Masterson *et al.* at $T_\pi = 143$ (Ref. 8) and 256 MeV (Ref. 9) are included for comparison. The data from the present experiment have several symbols associated with them to delineate results acquired during a given sequence from results acquired during a different sequence (this distinction is also made in Table II). As described in Sec. III, data are acquired at six angles simultaneously in this experiment for each sequence of alternating beam polarities.

At $T_\pi = 143$ MeV, the results from two sequences of measurements from the present experiment agree nicely with each other. The data reflect a flat angular distribution of $A(143, \theta)$ with values $\sim -1.5\%$. The results from this experiment are, however, inconsistent with those from Ref. 8, which consist of values around $+1$ to $+2\%$ in this angular region. The difference is more than can be accounted for by the experimental uncertainties.

The results of Masterson *et al.*^{8,9} are, however, dependent on the detailed $\pi^\pm p$ cross sections that were used to normalize their $\pi^\pm d$ data. Their original values of $A(T_\pi, \theta)$ at both 143 and 256 MeV were based on the $\pi^\pm p$ data of Bussey *et al.*,¹⁶ used in conjunction with the computer code SCATPI.¹⁷ Since publication of the CSB papers by Masterson *et al.*,^{8,9} there have been several recent $\pi^\pm p$ cross section measurements published, including one¹⁸ that employed techniques similar to those used in the present experiment. These new $\pi^\pm p$ measurements

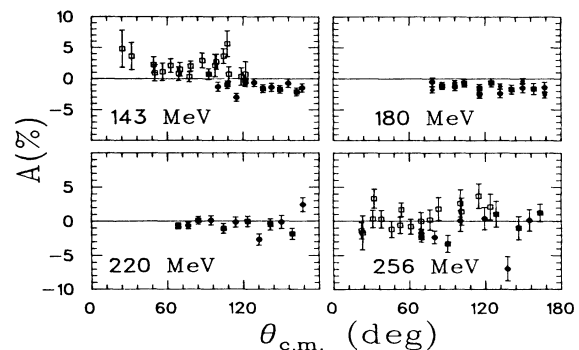


FIG. 4. The results of this experiment at $T_\pi = 143, 180, 220,$ and 256 MeV are shown (solid symbols). The original data of Masterson *et al.* are also shown at $T_\pi = 143$ (Ref. 8) and 256 MeV (Ref. 9) (open symbols). The charge asymmetry is plotted on the vertical axis in percent, the horizontal axis is the c.m. angle in degrees.

were undertaken to resolve discrepancies observed in the existing $\pi^\pm p$ data base.^{16,19,20,21} Arndt generated a new set of πN shifts (SP87) based on the data of Brack *et al.*¹⁸ as well as many of the other data sets. The $\pi^\pm p$ cross sections calculated from the SP87 phase shifts were used to renormalize the data of Masterson *et al.*^{8,9} These renormalized data appear in Fig. 5 (as well as in Figs. 6 and 8). Note that in Fig. 5 we have averaged the data of Ref. 8 where more than one measurement was made at the same angle. While there were only minor changes at 256 MeV, the 143 MeV data changed considerably, yielding values of $A(143, \theta)$ that were predominantly negative and in substantial agreement with the data of the present study. We stress that the present experiment is an absolute measurement of $A(T_\pi, \theta)$ requiring no normalization to $\pi^\pm p$ data. There remains some semblance of a bump in the renormalized data of Refs. 8 and 9 at about 110° but it is not statistically significant and there is no evidence for such a bump in the present data. The agreement between the $A(143, \theta)$ measurements of this experiment and those of Ref. 8 when normalized to the recent $\pi^\pm p$ data of Ref. 18 shows internal consistency between all three of these measurements.

The results of the present experiment at $T_\pi = 180$ MeV are also shown in Fig. 4. Three sequences of measurements were undertaken at this bombarding energy. All are consistent with one another. Two of the sequences were acquired by varying slightly the slits of the *M11* channel, in order to obtain fluxes of approximately 3.1 MHz for π^+ and 2.3 MHz for π^- . The third sequence was acquired by varying the *M11* intensity slits much more drastically, such that the π^+ and π^- fluxes were identical at 1.6 MHz. The angular distribution of $A(T_\pi, \theta)$ at this bombarding energy is flat, with values again near -1.5% . The shape and magnitude of $A(180, \theta)$ is very similar to $A(143, \theta)$.

At a bombarding energy of 220 MeV, the values of $A(220, \theta)$ move closer to zero. The angular distribution is again flat. The two sequences of measurements are in close agreement with one another.

At $T_\pi = 256$ MeV, the quality of data in both experiments has deteriorated. The results of the present experiment are generally consistent with those of Ref. 9 at an-

gles greater than 100° . Between 70° and 100° the two experiments disagree. The asymmetries measured in the experiment of Masterson *et al.*⁹ rise from near zero to around 3% in this angular region, whereas those of the present experiment fall from around -2% to -3% . Given the size of the experimental uncertainties in both experiments, however, the impact of this discrepancy may not be significant. Most disturbing is the datum from the present experiment at 137.5° , which lies between two and three standard deviations lower than where expected, based on the neighboring data. A detailed analysis offered no experimental explanation why $A(256, 137.5^\circ)$ has such a negative value, which is presumed to be a statistical fluctuation or an instrumental problem. The problems noted above may be considered a reflection of the fact that at this bombarding energy, not only has the differential cross section fallen by almost a factor of twenty from $T_\pi = 143$ MeV, but the ratio of π^- to π^+ incident flux has fallen drastically as well. These factors combined make the $A(T_\pi, \theta)$ measurements at higher energies especially challenging.

The general angular trend of $A(256, \theta)$ is negative (-2% to -3%) at forward angles, with a transition to slightly positive values ($\sim 1\%$) at backward angles. The slope and angular location of this transition is different for the two experiments.

Although the $\pi^\pm p$ data of Ref. 18 extend only to $T_\pi = 139$ MeV, due to the apparent superiority of the SP87 phase shifts at 143 MeV, we have used this new set of phase shifts to renormalize the 256 MeV data of Ref. 9 as well. In contrast to the situation at 143 MeV, the renormalization at 256 MeV has no significant impact on the earlier data of Ref. 9.

V. THEORETICAL TREATMENT

The electromagnetic perturbations which break charge symmetry are simple in principle, yet there are no methods to include them exactly in calculations of the scattering of a particle on a composite system. Approximations have to be invoked, and all face the same intrinsic problem, namely, a tiny differential measure— $A(T_\pi, \theta)$ —has to be calculated with corresponding accuracy. One has to determine which effects approximately cancel, and which are dominant in $A(T_\pi, \theta)$. This dilemma explains the variety of approximations which have been proposed^{8,10,12,9,22,23} trying to do partial justice to selected aspects of the problem. The latter difficulty is not of a fundamental nature, but one of precision.

Most methods make use of the global parameters C_M and C_Γ in Eq. (1) as a measure for CSB. Nonzero values of C_M or C_Γ indicate CSB. Of course, $C_M = C_\Gamma = 0$ corresponds to CS of the strong interaction, but the converse is not true. One obviously can have unequal mass and width parameters and still have $C_M = C_\Gamma = 0$. The use of these global parameters is thus seen to introduce a deficiency.

The approach of Ref. 22 just permits CSB on the level of each individual (3,3) channel. We recall here only its salient points. One writes the elastic amplitude in the form

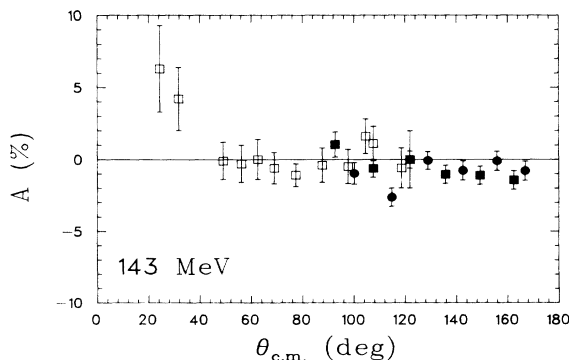


FIG. 5. The data of Ref. 8 renormalized using the SP87 phase shifts based on the recent $\pi^+ p$ data of Ref. 18 are shown (open symbols). The data of this experiment are also plotted (solid symbols) for comparison.

$$f_{\pi d} = f_{c,\text{ext}} + f_{c,s}^{\text{CSB}}. \quad (5)$$

In this expression, $f_{c,\text{ext}}$ is the external Coulomb amplitude for scattering of extended pion and deuteron charge distributions, and accounts for the observed (longitudinal) form factors.²⁴ There does not exist a closed form for the Coulomb modified, CSB strong amplitude $f_{c,s}^{\text{CSB}}$ in Eq. (5). Here, as was done in Ref. 22, we shall assume

$$f^{\text{CSB}} \approx (f - f_{\Delta}^{(2)})^{\text{CS}} + (f_{\Delta}^{(2)})^{\text{CSB}}. \quad (6)$$

In Eq. (6), $(f - f_{\Delta}^{(2)})^{\text{CS}}$ is the difference between the total charge symmetric amplitude and its dominant, second-order part. The latter we assume to be dominated by the CS (3,3) channel. The term $(f_{\Delta}^{(2)})^{\text{CSB}}$ in Eq. (6) is the CSB amplitude, which (for πd scattering) requires information on four different $(\pi N)_{T_i}$ channels. We also include in this term the p, n mass difference and moreover account for internal Coulomb effects between charged particles in intermediate states, not inherent in the CSB $(\pi N)_{T_i}$ amplitudes.

Actually, one cannot accurately calculate the CSB amplitude $(f^{(2)})^{\text{CSB}}$ in Eq. (6) because of lack of the required information on the off-shell πN amplitudes in the different charge states T_i . In Ref. 22 actual data for $\pi^+ p$ were utilized; for the remaining Δ_i , a scheme was suggested which produces amplitudes with given resonance masses M_i and widths Γ_i . Even these input elements are not all available. All widths with the exception of Γ_{++} are not, or at best poorly known.⁶ For the calculation reported in Ref. 22, for instance, a measured value²⁵ of $M_- - M_{++}$ was used, which leads to a large, and consequently strong CSB value for M_- . That value remains unconfirmed till today.

We thus need a judgement on the quality of resonance parameters. In Ref. 22 the values of Ref. 6 were taken, which correspond to $C_M = 6.6$ and $C_{\Gamma} = 5.2$ MeV. These numbers are now considered to be on the high side. Here, we still take the $(++)$ and $(+)$ parameters to be best known. Then first keeping M_0 and Γ_0 fixed, we scan C_M and C_{Γ} regions by varying M_- and Γ_- . We also

consider an alternative Γ_0 value to see its influence.

Although we have calculated the asymmetry function $A(T_{\pi}, \theta)$ for wide ranges of Γ_0 , C_M , and C_{Γ} , we shall confront all but the $T_{\pi} = 220$ MeV data with $(\Gamma_0, C_{\Gamma}) = (115.7, 3.5)$ MeV and $(112.6, 2.5)$ MeV. In both cases we tested $C_M = 2.5, 3.5,$ and 4.5 MeV. $A(143, \theta)$ has also been calculated with $C_M = 4.5$ MeV, $C_{\Gamma} = 1.2$ MeV, and $\Gamma_0 = 112.6, 115.7$ MeV. The specific combinations of parameters we have investigated are tabulated in Table III.

The results, displayed in Figs. 6, 7, and 8, show that the sensitivity of $A(T_{\pi}, \theta > 70^\circ)$ to changes in Γ_0 , C_M , and C_{Γ} is greatest for 143 MeV, less for 256 MeV, and rather small for $T_{\pi} = 180$ MeV. Obviously, the range of input parameters can only be limited if the data fall within the spread of the predicted $A(T_{\pi}, \theta)$, and if the spread is large compared to the experimental uncertainties. These conditions are met only for $T_{\pi} = 143$ MeV.

At $T_{\pi} = 256$ MeV, the present calculations are compared to the existing data in Fig. 6. The present and older⁹ predictions, which are not very sensitive to the choice of parameters, agree reasonably well with each other. The older data at this bombarding energy,⁹ extending down to $\theta \sim 22^\circ$, roughly correspond to the predicted $A(256, \theta)$. None of the calculations predict the negative values of $A(256, \theta)$ measured in the present experiment at 79.9° and 90.3° , which are moreover in disagreement with the earlier experiment of Masterson *et al.*⁹ Due to the large experimental uncertainties of both experiments, coupled with the insensitivity of the predictions to the choice of parameters, a determination of mass or width parameters has not been attempted at this bombarding energy. The analysis of Masterson *et al.*⁹ at this bombarding energy favored values of C_M between 2.0 and 4.5 MeV. Although there was little sensitivity to C_{Γ} in their analysis, their preferred value for C_{Γ} was 2.33 MeV. Beyond 100° the present data are slightly overpredicted with these mass and width parameters. At the present time, no calculations are available at $T_{\pi} = 220$ MeV.

At $T_{\pi} = 180$ MeV our data for $A(180, \theta > 78^\circ)$ occupy a band around $\sim -1.5\%$. The present predictions all cluster around $A(180, \theta) \sim 0$ to -0.5% in the backward

TABLE III. The resonance parameters used for the calculations shown in Figs. 6, 7, and 8 are shown. All numbers are in MeV. Fixed values (Ref. 6) are $M_{++} = 1231.1$, $M_+ = 1230.5$, $M_0 = 1232.5$, $\Gamma_{++} = 111.5$, and $\Gamma_+ = 113.5$ MeV.

Solution	C_M	C_{Γ}	M_-	Γ_0	Γ_-
1	4.5	3.5	1234.9	115.7	113.3
2	3.5	3.5	1233.9	115.7	113.3
3	2.5	3.5	1232.9	115.7	113.3
4	4.5	2.5	1234.9	112.6	114.3
5	3.5	2.5	1233.9	112.6	114.3
6	2.5	2.5	1232.9	112.6	114.3
7	4.5	1.2	1234.9	112.6	113.0
8	4.5	1.2	1234.9	115.7	112.0

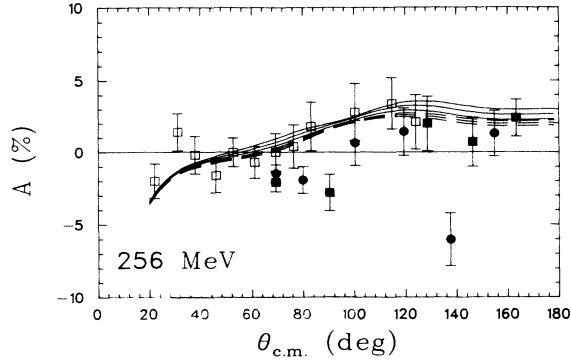


FIG. 6. The $T_\pi=256$ MeV data from the present experiment (solid symbols) as well as the renormalized data of Ref. 9 (open symbols) are shown. The present calculations are shown for $C_\Gamma=3.5$ MeV (solid curves) and $C_\Gamma=2.5$ MeV (dashed curves). For a given choice of C_Γ , successively more positive $A(T_\pi, \theta)$ values are predicted as C_M assumes the values 2.5, 3.5, and 4.5 MeV.

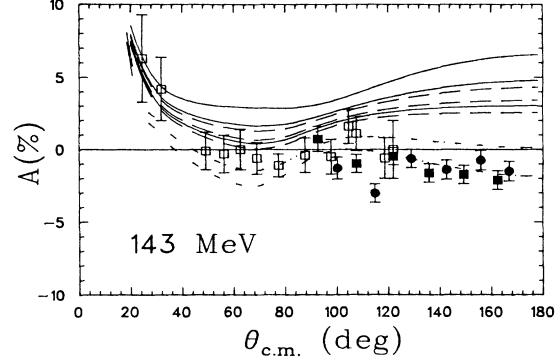


FIG. 8. The $T_\pi=143$ MeV data from the present experiment (solid symbols) are shown, as well as the renormalized older data from Ref. 12 (open symbols). The present calculations are shown for $C_\Gamma=3.5$ MeV (solid curves) and $C_\Gamma=2.5$ MeV (dashed curves). For a given choice of C_Γ , successively more positive $A(T_\pi, \theta)$ values are predicted as C_M assumes the values 4.5, 3.5, and 2.5 MeV. The dashed-dotted curves correspond to solutions 7 (upper curve) and 8 (lower curve) from Table III.

hemisphere, as shown in Fig. 7. The negative excursion predicted for $A(180, \theta \sim 80^\circ)$ in Ref. 22 becomes less pronounced for the set of parameters chosen here. No such structure emerges in the calculations of Ref. 10 which moreover predict small positive values (between 0 and 2%) for $A(180, \theta \geq 50^\circ)$ for all mass and width parameters considered. The tight clustering of the theoretical predictions for all parameter sets employed again renders pointless the extraction of mass and width parameters at this bombarding energy. Although the discrepancy between the present and earlier¹⁰ calculations is only about 1% (except for the negative excursion predicted in the present calculations near 70°), the data favor the present calculations.

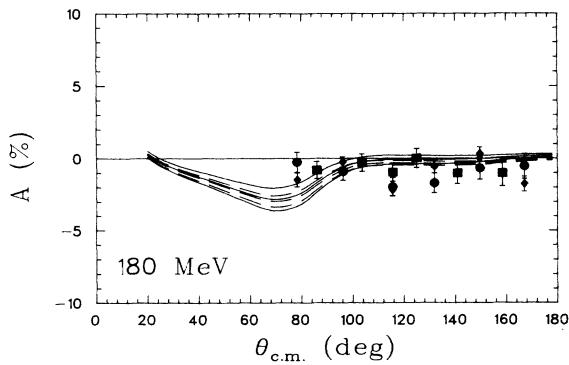


FIG. 7. The $T_\pi=180$ MeV data from the present experiment (solid symbols) are shown. The present calculations are shown for $C_\Gamma=3.5$ MeV (solid curves) and $C_\Gamma=2.5$ MeV (dashed curves). For a given choice of C_Γ , successively more positive $A(T_\pi, \theta)$ values are predicted as C_M assumes the values 4.5, 3.5, and 2.5 MeV.

At $T_\pi=143$ MeV the situation is summarized in Fig. 8. The calculations show the desired sensitivity to the parameters at this bombarding energy, enabling a reliable determination of C_M and C_Γ . As described earlier, the present data at this energy cluster around $A(143, \theta) \sim -1.5\%$, in agreement with the renormalized older data of Ref. 8. The present calculations with $C_\Gamma=3.5$ or 2.5 MeV all predict positive values of $A(143, \theta)$ regardless of the value of C_M . Only the predictions for $C_\Gamma=1.2$ MeV produce the negative $A(143, \theta > 60^\circ)$ values observed experimentally. The shape of the predictions is such that it is difficult to describe simultaneously the older, forward angle data of Ref. 8 and the predominantly backward angle data of the present experiment. Given the problems discussed above concerning the $\pi^\pm p$ renormalizations and radiative corrections to the older data, we prefer parameter set eight from Table III, which appears to provide the best description of the data from the present experiment at this bombarding energy, even though the (renormalized) data of Ref. 8 are slightly underpredicted. This parameter set has identical C_M and C_Γ values (4.5 and 1.2 MeV, respectively) as parameter set 7, but different combinations of the widths Γ_0 and Γ_- . The combination $\Gamma_0=115.7$ MeV and $\Gamma_-=112.0$ MeV seems preferred by comparison to the present data.

Previous calculations^{8,9} are reasonably consistent with this choice of parameters, showing a preference for $C_M=3.1$ MeV, and $C_\Gamma=1.24$ MeV when compared to our experimental results and the renormalized data of Ref. 8.

Although the present and older calculations demonstrate great sensitivity to the mass and width parameters, and moreover point to similar values for C_M and C_Γ , there are disturbing differences between the predictions given the same choice of parameters. For example, the calculations of Masterson *et al.* at 143 MeV,⁹ with

$C_M=4.47$ MeV and $C_\Gamma=1.24$ MeV are flat in the backward hemisphere (as are the data), rising monotonically with decreasing angle inside of about 100° . The present calculations, using the same values for C_M and C_Γ , predict structure near 100° and only begin to rise inside of 60° . The magnitude of both predictions is similar [for example both predict $A(143, 180^\circ) = -2\%$]. Other examples (again at 143 MeV), however, have similar shapes but different magnitudes. Using $C_M=4.47$ MeV and $C_\Gamma=3.6$ MeV, Masterson *et al.* predict asymmetries near zero in the backward hemisphere whereas those of the present study, for the same choice of parameters and in the same angular region, are closer to 3%. The reasons for these discrepancies are not understood. We attribute the fair agreement between mass and width parameters extracted using the two calculations to the great sensitivity to these parameters at this bombarding energy.

The values of C_M determined from both theoretical prescriptions are also consistent with the value of C_M obtained from the total cross section measurements of Ref. 7, although the reported C_Γ there is larger than the value we find. The value for the mass parameter determined from our analysis ($C_M=4.5$ MeV) is furthermore in good agreement with that predicted from a bag model calculation of Bickerstaff and Thomas²⁶ ($C_M=4.55$ MeV).

VI. CONCLUSIONS

Measurements of the charge asymmetry $A(T_\pi, \theta)$ in elastic πd scattering have been made at bombarding energies of $T_\pi=143, 180, 220,$ and 256 MeV. For $T_\pi=180$ and 220 MeV these are the first measurements. The results for $T_\pi=256$ MeV are consistent with those of an earlier experiment⁹ in the backward hemisphere, but differ slightly in the angular region between 70° and 100° . At $T_\pi=143$ MeV, the results of the present experiment agree nicely with those of Masterson *et al.*⁸ provided the earlier data are renormalized to new, more precise $\pi^\pm p$ data.¹⁸ This renormalization also causes the enigmatic bump⁸ in $A(143, \sim 100^\circ)$ practically to disappear in accordance with the present experiment.

At $T_\pi=256$ MeV, both theoretical prescriptions studied here do reasonably well describing the existing data. Measurements at two angles from the present study at 79.9° and 90.3° fall outside the band defined by all predictions, as does the datum at 137.5° . Unfortunately, at this bombarding energy the larger experimental uncertainties

associated with the $A(T_\pi, \theta)$ measurements, coupled with the predicted insensitivity to different mass and width parameters, makes the extraction of reliable values for C_M and C_Γ difficult at best.

At $T_\pi=180$ MeV, both theoretical prescriptions considered here predict tight clustering of $A(180, \theta)$ for all parameters considered. The present predictions lie about 1% lower than those of Masterson,¹⁰ in better agreement with the data. The structure predicted by the present calculations at forward angles is not predicted by Masterson, and the angular range of the data is insufficient to discriminate between the two calculations in this region.

By far the most interesting data are those for $T_\pi=143$ MeV. Great sensitivity to values of a presently preferred choice of resonance parameters permits the extraction of $C_M=4.5$ MeV, $C_\Gamma=1.2$ MeV, and a preference for $\Gamma_0=115.7$ MeV. The C values are close to those extracted in Ref. 9, namely, $C_M=4.5$ MeV, $C_\Gamma=1.24$ MeV, even though we have presented arguments which suggest that the data from that experiment were incorrectly normalized. Furthermore, the C values extracted from this study are consistent with those from total cross-section measurements. The mass parameter C_M found in this study is also in agreement with that predicted from a bag model calculation of the up-down quark mass difference.²⁶

We repeat that the C parameters are global ones which do not distinguish between different M_i, Γ_i values for the individual Δ_i leading to the same C_M and C_Γ . One can well imagine that a second generation of data will put sharper bounds on what is in reality a many parameter situation. It goes without saying that greater experimental precision will demand corresponding attention to neglected details of the calculations. In any event it is not possible on the basis of the present data to set limits (uncertainties) on the C parameters and the lesser known mass and width parameters for Δ_i .

ACKNOWLEDGMENTS

We gratefully acknowledge the help of the TRIUMF technical and support staff, as well as the financial support of the Natural Sciences and Engineering Research Council of Canada. We also thank M. Kohler and V. Li for assistance with the data analysis. This work was supported in part by the U.S. DOE.

*Permanent address: University of Trieste, Trieste, Italy.

¹G. R. Smith *et al.*, Phys. Rev. C **29**, 2206 (1984).

²G. R. Smith *et al.*, Phys. Rev. Lett. **57**, 803 (1986).

³R. J. Holt *et al.*, Phys. Rev. Lett. **43**, 1229 (1979); **47**, 472 (1981); E. Ungricht *et al.*, *ibid.* **52**, 333 (1984); E. Ungricht *et al.*, Phys. Rev. C **31**, 934 (1985).

⁴J. Ulbricht *et al.*, Phys. Rev. Lett. **48**, 311 (1982); W. Gruebler *et al.*, *ibid.* **49**, 444 (1982); V. Koenig *et al.*, J. Phys. G **9**, L211 (1983); Swiss Institute for Nuclear Research Annual Reports, p. NL 18, 1984 (the validity of these measurements has

been questioned—see Ref. 2).

⁵Y. M. Shin *et al.*, Phys. Rev. Lett. **55**, 2672 (1985).

⁶F. Myrher and H. Pilkuhn, Z. Phys. A **276**, 29 (1976); Phys. Rev. **170B**, 1 (1986).

⁷E. Pedroni *et al.*, Nucl. Phys. **A300**, 321 (1978).

⁸T. G. Masterson *et al.*, Phys. Rev. Lett. **47**, 220 (1981); T. G. Masterson *et al.*, Phys. Rev. C **26**, 2091 (1982).

⁹T. G. Masterson *et al.*, Phys. Rev. C **30**, 2010 (1984).

¹⁰T. G. Masterson, Phys. Rev. C **31**, 1957 (1985).

¹¹B. Balestri *et al.*, Nucl. Phys. **A392**, 217 (1983).

- ¹²J. Frohlich, B. Saghai, C. Fayard, and G. H. Lamot, Nucl. Phys. **A435**, 738 (1985).
- ¹³C. Ottermann *et al.*, Phys. Rev. C **32**, 928 (1985).
- ¹⁴E. Borie, Phys. Lett. **68B**, 433 (1977); E. Borie, Z. Naturforsch. **33a**, 1436 (1978).
- ¹⁵M. R. Sogard, Phys. Rev. D **9**, 1486 (1974).
- ¹⁶P. J. Bussey *et al.*, Nucl. Phys. **B58**, 363 (1973).
- ¹⁷SCATPI, a computer code for calculating πN cross sections and polarizations for incident pion energies between 90 and 300 MeV; J. B. Walter and G. A. Rebka, Los Alamos Report UC34A, 1979 (unpublished).
- ¹⁸J. Brack *et al.*, Phys. Rev. C **34**, 1771 (1986).
- ¹⁹P. Y. Bertin *et al.*, Nucl. Phys. **B106**, 341 (1976).
- ²⁰B. G. Ritchie *et al.*, Phys. Lett. **125B**, 128 (1983).
- ²¹J. S. Frank *et al.*, Phys. Rev. D **28**, 1569 (1983).
- ²²A. S. Rinat and Y. Alexander, Nucl. Phys. **A404**, 467 (1983).
- ²³R. Rockmore and B. Saghai, Phys. Rev. C **28**, 2064 (1983).
- ²⁴S. M. Amendolia *et al.*, Nucl. Phys. **B277**, 168 (1986); S. Galster *et al.*, *ibid.* **32**, 221 (1971); C. G. Simon, Ch. Schmitt, and V. H. Walther, *ibid.* **A364**, 285 (1981).
- ²⁵L. G. Dakhno, *et al.*, Yad. Fiz. **33**, 112 (1981) [Sov. J. Nucl. Phys. **33**, 59 (1981)].
- ²⁶R. P. Bickerstaff and A. W. Thomas, Phys. Rev. D **25**, 1869 (1982).